

Performance Analysis of Turbocharger

S. Sowmya¹, L. S. V. Prasad²

¹Thermal Engineering, Andhra University, Visakhapatnam, India

²Department of Mechanical Engineering, Andhra University, Visakhapatnam, India

ABSTRACT

Turbochargers have found a prominent place in recent engines enhancing power without much increase in weight. The future trends of automotive engine are universally toward down-sizing, higher power, lower emissions and above all overall efficiency of the engine. Among many technologies revolutionizing automotive development, turbo charging is considered as a significant enabler to meet the ever increasing future demands. Blades are modelled using CATIA and ANSYS for various inlet blade angles and back swept angles. Analysis reveals that for an inlet blade angle of 50° with swept back angle of 30° the turbocharger yielded higher efficiency. The materials considered for the analysis are Inconel 740 and Mar M 247.

Keywords: Turbocharger, Thermal Analysis

I. INTRODUCTION

Turbocharger is an air pump designed to operate on the normally wasted energy in engine exhaust gas. These gases drive the turbine wheel (hot wheel) and shaft which is coupled to a compressor wheel (cold wheel) which when rotating provides high volume of air to the engine combustion chambers. Exhaust gases, going out from an engine through an exhaust manifold, are directed to a turbine chamber where a rotor is situated. By means of a shared shaft, it drives compressor's rotor located on the other side of the device (frequently referred to as "cold"), which compresses the air supplying the engine. Since compressed air includes more oxygen in one volume unit, it is possible to create better conditions for the combustion process. Increased oxygen amount with additional amount of fuel can be used to increase engine power, or as with diesel engines, it facilitates more complete combustion, reducing the amount of emitted contamination and boosting its efficiency. Increasing air compression in the same volume, at the same time, its temperature is increased. Higher temperature is connected with lower density, which means that cylinders receive the amount of oxygen smaller than if the air temperature were lower. Therefore, a charging air radiator (intercooler) is used as shown in Fig. 1.

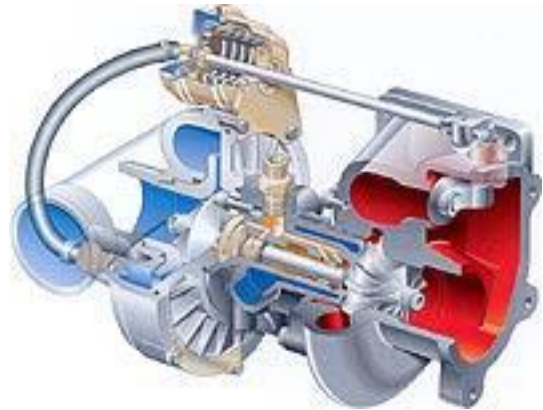


Figure 1: Turbocharger Section View

II. MODELLING AND ANALYSIS OF 1D BLADE

Vista CCD is a software which is commonly used for the preliminary design of centrifugal compressors. Vista CCD is used in an iterative fashion to create a 1D design of components selected for the study. An accurate 1D model can provide an insight into the performance of the machine that goes beyond the test measurements. As the blades are symmetrical in design, a single turbine blade is generated using Vista CCD as shown in Fig. 2. Analysis discussed in this paper is correspondingly for an inlet blade angle of 50° with swept back angle of 30° .

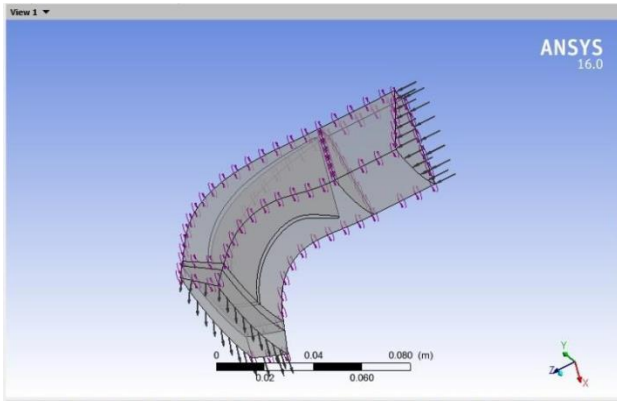


Figure 2: Blade and Domain with Loading and Rotation

The design specifications of the turbine blade are as follows.

- No. of blade = 10
- Hub diameter = 25mm
- Shroud diameter = 81 mm
- Height of blade = 20mm

The blade design parameters considered for Vista CCD analysis are presented in Table 1. A single table is presented for the sake of convenience.

Nomenclature

- Young's Modulus - E
- Thermal Conductivity -k
- Thermal exp. Coeff. - α
- Mass Density - ρ
- Poission's Ratio - ν
- Specific Heat -Cp
- Mach nuber -U/C

Table.1: Blade Designing Parameters

| | | | |
|--------------------|---------------|-------------------------|----------------------|
| Pressure ratio | 2.5 | Inlet tip diameter | 90mm |
| Speed | 80000 rev/min | Inlet blade height | 20mm |
| Outlet pressure | 101325 Pa | Exducer tip diameter | 81mm |
| Inlet temperature | 873K | Exducer hub diameter | 25mm |
| Mass flow rate | 0.5Kg/s | Exducer RMS blade angle | 45 ° |
| Rotor blade number | 10 | Exducer throat area | 2740 mm ² |

The complete model of turbine in a turbocharger developed using CATIA as shown in Fig. 3. The parasolid model is subjected for meshing, Tetrahedron meshing is selected with total number of nodes and elements of 24139 and 13178 respectively as shown in Fig. 4.

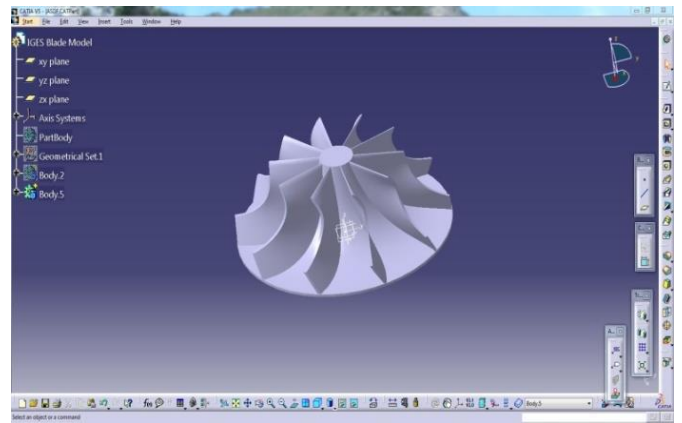


Figure 3 : Geometry Created in CATIA

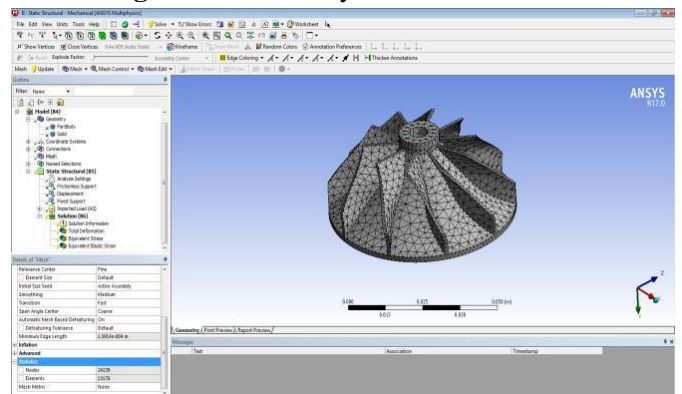


Figure 4: Meshed model of Turbine

As the turbine in a turbocharger is exposed to high temperatures, suitable materials have to be selected to with high heat resistance and corrosion resistance [3]. Two different materials namely Inconel and Mar M 247 are selected for the analysis and their respective properties are presented in Table. 2.

Table 2: Material properties of Inconel and Mar M 247

| Property | Symbol | Units | Mar-M 247 | Inconel 740 |
|----------------------|----------|---------------------------------|-----------|-------------|
| Young's Modulus | E | G Pa | 220.24 | 221 |
| Thermal Conductivity | k | W/mK | 7.29 | 10.5 |
| Thermal exp. Coeff. | α | 10 ⁶ K ⁻¹ | 6.34 | 6.8 |
| Specific Heat | Cp | J/kgK | 418.6 | 251 |
| Poission's Ratio | ν | - | 0.3 | 0.28 |
| Mass Density | ρ | Kg/m ³ | 8525.4 | 8050 |

III. VALIDATION OF PRESENT ANALYSIS

The parasolid model developed using Vista CCD is subjected to boundary conditions Liam Barr et al.[2]. The results obtained are tabulated in Table 3. The validation is carried out for two different rotating speeds namely 50,000 rpm and 80,000 rpm with U/C ratio of 0.38 and 0.6 respectively. The efficiency of turbocharger estimated from analysis was found to be in close agreement with values published in literature [2].

Table 3: Efficiency Comparison at Different RPM

| Blade shape | Efficiency at RPM 50000 | | Efficiency at RPM 80000 | |
|----------------|-------------------------|------------------|-------------------------|------------------|
| | Liam Barr et al.[2] | Present analysis | Liam Barr et al.[2] | Present analysis |
| Radial | 50 | 50.6 | 50 | 53.6 |
| 15° back swept | 51 | 52 | 51 | 51.9 |
| 30° back swept | 55 | 54 | 52 | 50.13 |

Further as the results were found to be in close agreement, the analysis is extended to study the influence of inlet flow angles on performance of turbocharger. Three different inlet blade angles namely 40°, 45° and 50° were selected for the study and the detailed analysis for 50° inlet blade angle is presented in the subsequent sections.

IV. RESULTS AND DISCUSSION

The static pressure distribution along the length of the turbine blade is shown in Fig. 5. The pressure distribution is found to be higher at the tip of the turbine blade as the exhaust gas strikes the blade in a tangential direction rotating the turbine blade and later flows through the exhaust gate valve to the ambient. The pressure is found to be marginally less near the hub region of the turbine rotor as compared at the inlet.

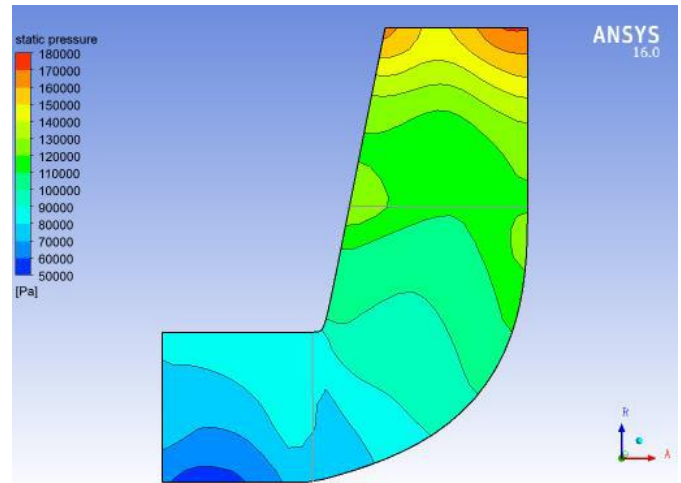


Figure 5. Static pressure distribution along the blade

The meridional contour for a turbine blade for Mach number is found to vary significantly along the turbine blade as shown in Fig 6. Mach number is found to be higher at the entry portion of the turbine blade as compared to the central hub of the rotor. The Mach number is found to be supersonic at the entry zone and subsides significantly to subsonic near the hub. At Mach numbers much less than 1.0, compressibility effects are negligible and the pressure variation caused by gas density can be safely ignored in flow modelling [1]. The exhaust gas velocity striking the turbine blade could vary significantly along the turbine rotor while the turbine spins at same speed irrespective of the exhaust gas striking any part of the turbine inside the shroud.

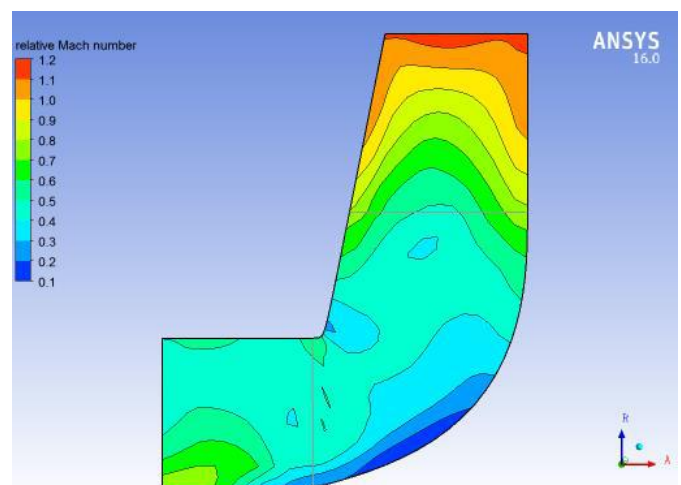


Figure 6. Meridional contour of Mach number along the blade

The flow properties analysed along interspatial turbine blades selected for the study are presented in the subsequent sections. Fig. 7 shows localized variation of Mach number at the root of the interspatial blades

attached to the turbine wheel. It is found to be more symmetric in nature without any localized vortices. The Mach number is found higher, where the exhaust gases strike the blade first and then drops as it flows across the turbine blade. Further, Fig. 7 shows no evidence of shock wave generated at the entry region of the turbine blade.

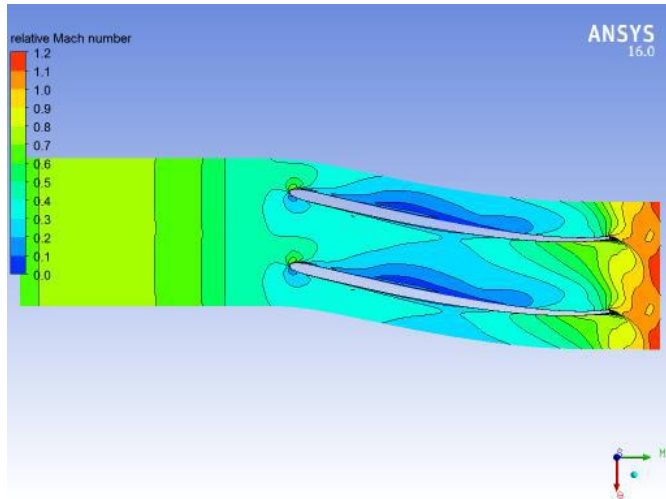


Figure 7. Interspatial variation of Mach number at root of blade

Variation of Mach number along the tip of the turbine blade across the turbocharger is shown in Fig. 8. The Mach number is found to vary extensively along the interspatial tip of the turbine blade. The Mach number in proximity to the blade tip are found to be relatively higher with certain localized spots indicating very low Mach number probably due lack of flue gas moment at certain interspatial locations.

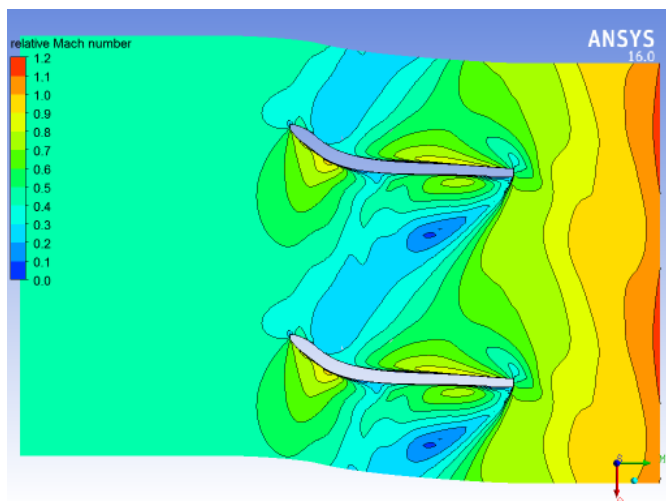


Figure 8. Interspatial variation of Mach number at tip of blade

The pressure distribution at the root of the turbine blades is shown in Fig. 9. The flue gas is found to strike

at the central part at the root of the turbine blade and the pressure locally is found to be 0.95 bar and found to further decreases along the radial direction as the flow proceeds across the turbine blade.

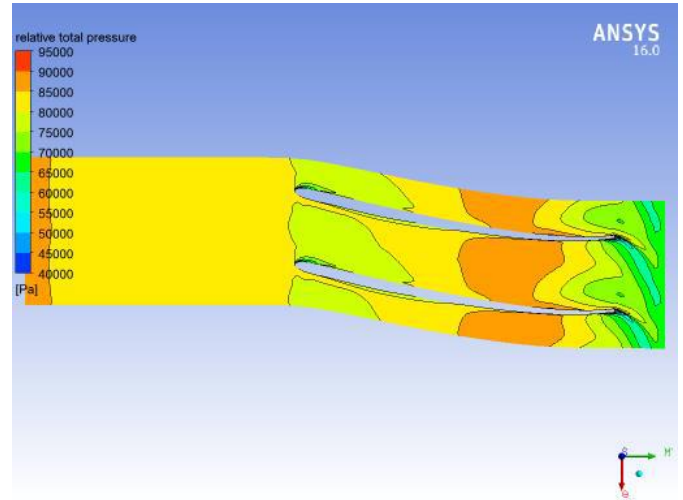


Figure 9. Pressure distribution at root of blade

The pressure distribution along the tip of the turbine blade is shown in Fig. 10. The pressure distribution is found to be higher at the interface of the turbine blade and the working fluid. A maximum pressure of 1.1bar is observed at the interface with certain localized minimal pressure spots observed at the interspatial locations at the tip of the turbine blades.

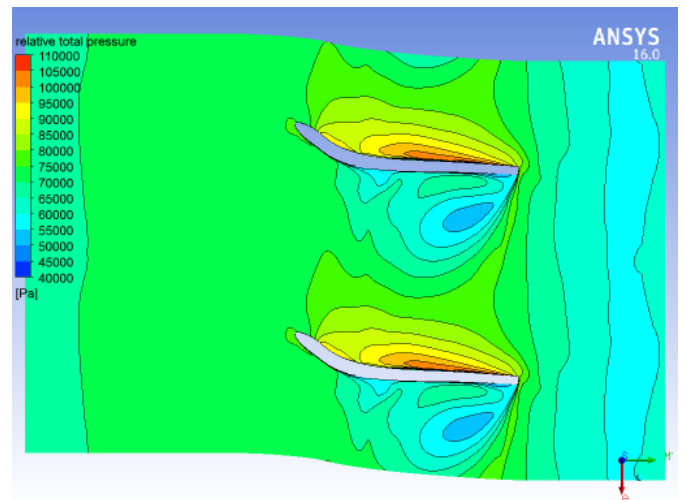


Figure 10. Pressure distribution at tip of turbine blade
International Journal of Scientific Research in Science, Engineering and Technology (ijsrset.com) 5

Velocity profile of flue gas striking at the root of the turbine blade is shown in Fig. 11. The velocity is found to be maximum at it strikes the turbine along the tangential direction imparting its momentum onto the rotor. A distinctive development of boundary layer can be observed along the turbine blade length with minimum velocity near the blade surface.

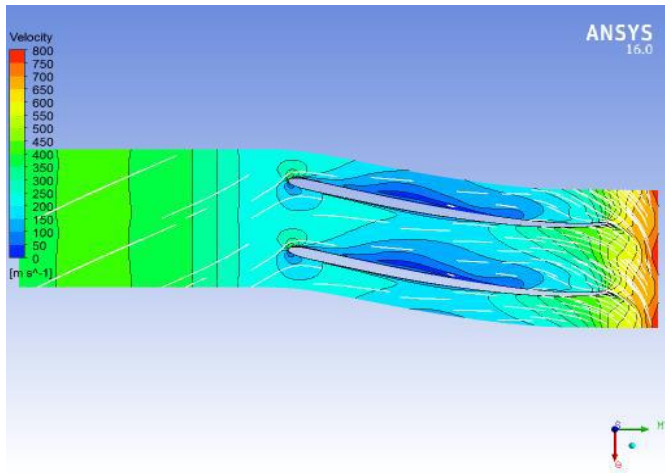


Figure 11. Velocity distribution at root of blade

The velocity profile of flue gas striking the turbine blade tip is shown in Fig. 12. The velocity of the flue gas is found to be maximum near the shroud and decreases at proximity of the blade tip. Moderate velocity distribution is observed near the blade tip and with reflective mass at the underside of the turbine blade.

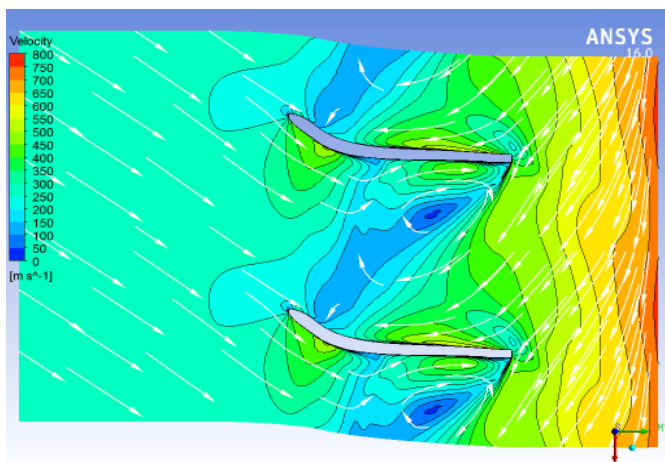


Figure 12. Velocity distribution along tip of turbine blade

An insight to interspatial analysis on pressure and velocity distribution in a turbocharger is extended to the complete turbine rotor for thermal analysis and equivalent stress distribution, which are also considered a priority is presented subsequently. The thermal analysis on the turbine of a turbocharger is shown in Fig. 13. The total deformation is found to be profoundly more circumferentially on the turbine. The flue gas striking the turbine contributes largely for higher deformation at the circumference and the deformation is found to decrease as the flue gas flows radially into the turbine. The maximum deformation was found to be 0.112m circumferentially.

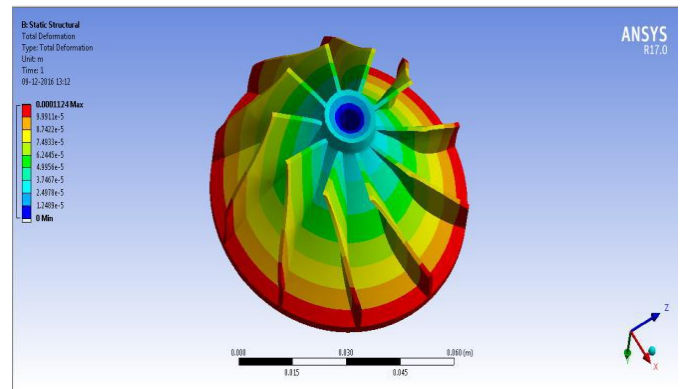


Figure 13. Total deformation for Mar M 247

Total deformation for Mar M 247 for same flow conditions is shown in Fig. 14. Similar trend in deformation is observed across the turbine for Mar M 247 with maximum deformation of 0.104m which is marginally less as compared to Inconel 740.

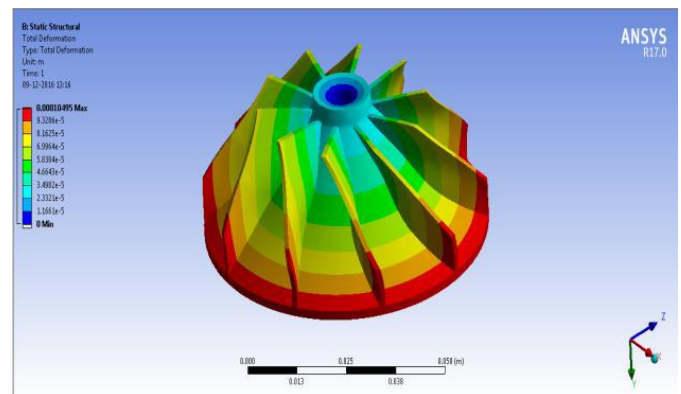


Figure 14. Total deformation for Mar M 247

The equivalent stress distribution for Inconel 740 is shown in Fig. 15. The equivalent stress developed is found to be almost uniform across the turbine with few concentrated locations near the hub. The maximum equivalent stress developed near the hub is estimated as 3.05 N/m².

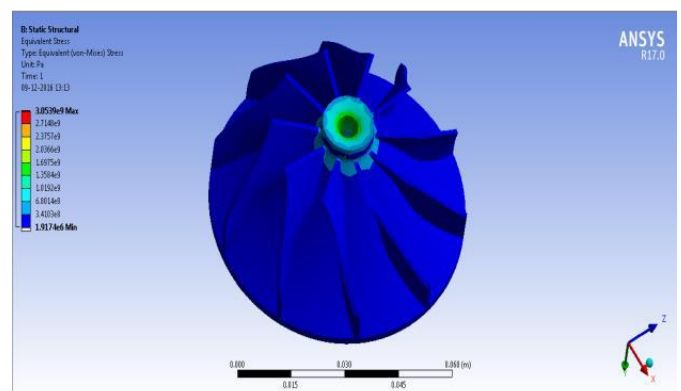


Figure 15. Equivalent stress contour for Inconel 740

The equivalent stress distribution for Mar M 247 is shown in Fig. 16. The equivalent stress developed under similar loading conditions was found to be uniform in trend as found for Inconel 740 and the maximum equivalent stress as estimated from the analysis is found to be 2.85 N/m², which is comparatively less as compared to Inconel 740

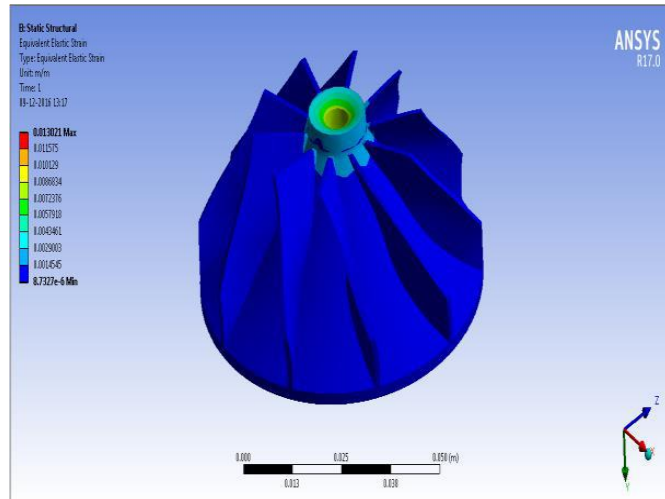


Figure 16. Shows contour of equivalent stress of Mar M 247

V. CONCLUSION

The relative performance of the turbocharger for various inlet blade geometries is summarized and shown in Fig. 17. A turbocharger with 50° inlet blade angle and 30° back swept angle is found to yield an optimum performance as compared to the rest of the geometry considered for the analysis. Further Mar M 247 is found to develop relatively lower equivalent stress as compared to Inconel 740.

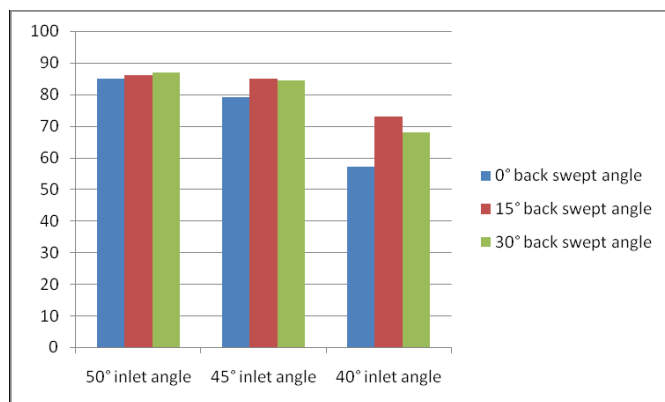


Figure 17. Turbocharger Efficiency for Various Blade Geometry

VI. REFERENCES

- [1]. Tie Wang, Cheng Peng, Jing Wu, . A journal on “Back swept angle performance analysis of centrifugal compressor”. ISSN 1392–1207. MECHANIKA. 2014 Volume 20(4): 402–406
- [2]. Liam Barr, MEng, AMIMEchE, Stephen W.T. Spence, CEng, PhD, MIMechE, MIEI, Tony McNally, PhD, BSc Queen’s University of Belfast, UK. A journal on “Numerical Study On Performance Characteristics Of Radial Turbine With Varying Blade Angles” in 8th International Conference Of Turbochargers And Turbocharging.
- [3]. URL as <http://allinoneblog.co.uk/turbocharger-construction-materials-working-conditions/>
- [4]. Mohd Muqem1, Dr. Mukhtar Ahmad2, Dr. A.F. Sherwani3. Turbocharging of Diesel Engine for Improving Performance and Exhaust Emissions: A Review IOSR Journal of Mechanical and Civil Engineering (IOSR-JMCE) e-ISSN: 2278-1684, p-ISSN: 2320-334X, Volume 12, Issue 4 Ver. III (Jul. - Aug. 2015), DOI: 10.9790/1684-12432229
- [5]. S. P. Shah1†, S. A. Channiwala2, D. B. Kulshreshtha1 and G. Chaudhari1. Journal of Applied Fluid Mechanics, Vol. 9, No. 4, pp. 1791-1798, 2016. ISSN 1735-3572, EISSN 1735-3645. Study of Flow Patterns in Radial and Back